Rheology of a Lower Critical Solution Temperature Binary Polymer Blend in the Homogeneous, Phase-Separated, and Transitional Regimes

M. Kapnistos,[†,‡] A. Hinrichs,[§] D. Vlassopoulos,*[,†] S. H. Anastasiadis,[†,‡] A. Stammer,[§] and B. A. Wolf[§]

Foundation for Research & Technology−Hellas, Institute of Electronic Structure & Laser, P.O. Box 1527, 71110 Heraklion, Crete, Greece, and Institut für Physikalische Chemie der Universität Mainz, Jakob-Welder Weg 13, D-55099 Mainz, Germany

Received June 7, 1996[⊗]

ABSTRACT: Small amplitude oscillatory shear rheology is employed in order to investigate the linear viscoelastic behavior of the lower critical solution temperature blend polystyrene/poly(vinyl methyl ether), PS/PVME, as a function of temperature and composition. At low temperatures, where the mixture is homogeneous, the dependence of the zero shear viscosity (η_0) on concentration is measured and is well-described by means of a new mixing rule, based on surface fractions instead of volume fractions. Shift factors from time-temperature superposition (TTS) exhibit a Williams−Landel−Ferry (WLF) behavior. As the macrophase separation temperature is approached (the phase diagram being established by turbidity measurements), the blend exhibits a thermorheologically complex behavior. A failure of TTS is observed at low frequencies, both in the homogeneous pretransitional and in the two-phase regimes. Its origin is attributed to the enhanced concentration fluctuations, which exhibit a critical slowing down near the phase boundary in the homogeneous regime, and in the two-phase morphology inside the phase-separated regime. The anomalous pretransitional behavior can be quantified using a recent mean field theory, yielding the spinodal temperature. Furthermore, in the two-phase region an intermediate region of enhanced moduli at low frequencies is observed, followed by flow at even lower frequencies, which is attributed to the two-phase structure. The linear viscoelastic properties of the phase-separated blends are, to a first approximation, adequately described by a simple incompressible emulsion model considering a suspension of droplets of one coexisting phase in the matrix of the other phase.

I. Introduction

The rheology of multicomponent systems, such as polymer blends and block copolymers, has long attracted the interest of the scientific and industrial community, due to the interesting physical problems and the ever-increasing technological applications.[1] Most of the work carried out to date addresses the rheological behavior of immiscible polymer blends,[2] frequently encountered during processing; such systems typically exhibit long relaxation times. The homogeneous region has received much less attention,[3−5] and in particular, the interesting regime in the vicinity of phase separation has become the subject of a limited number of investigations only recently.[4−6] Yet, the mechanisms contributing to the thermorheological complexity, reported when the homogeneous polymer blend phase separates, are not fully understood. Related to this problem is the question of the effects of shear on the phase behavior of polymer blends. The latter has been the subject of recent experimental[7] and theoretical[8] investigations; it is evident that accurate knowledge of the rheological behavior at a certain temperature near the phase separation will lead to a more accurate determination of the degree of enhanced miscibility (or demixing), ΔT (temperature difference), with respect to the quiescent phase diagram. Some of the specific questions which still remain unresolved include the following: (i) How do the linear viscoelastic properties change as the blend phase separates? (ii) Which are the differences between polymer blends and other multiconstituent systems, such as block copolymers, that have been studied extensively near their order−disorder transition?[9] (iii) How can the effects of phase separation on rheology be quantified? (iv) How can some controversial issues raised in the literature, namely, by the time-temperature superposition (or lack of it) of the loss modulus G'' [4,5] and the apparent plateau in storage modulus G' at low frequencies,[5a] be accounted for? (v) How can the rheology of a phase-separated system possessing large glass transition (T_g) contrast between its two constituents be described?

The above issues are addressed in this paper, which represents a systematic investigation of the linear viscoelastic properties of a binary polymer blend as a function of composition and temperature, i.e. from the homogeneous to the phase-separated regime. The system chosen, a mixture of polystyrene (PS) and poly(vinyl methyl ether) (PVME), is a lower critical solution temperature (LCST) blend that has been studied extensively in the past.[3−6,10] Nevertheless, the above questions mainly arise from the previous works with PS/PVME. Moreover, it is a good system to study rheologically in a wide temperature range, since, as will be discussed in the next sections, the suitable choice of component molecular weights leads to cloud points in the range of 100 °C while in the entangled state. Furthermore, its two components possess a large difference in T_g's and this is important because it provides significant "dynamic contrast" or "dynamic asymmetry", as it will become evident below. This asymmetry is thought to be responsible for the "viscoelastic phase separation" [11] in such blends.

This paper is organized as follows: molecular characteristics and experimental techniques are presented in the Experimental Section, section II. Then, section

* Author to whom correspondence should be addressed.
† Institute of Electronic Structure & Laser.
‡ Also at University of Crete, Physics Department, 71110 Heraklion, Crete, Greece.
§ Institute für Physikalishe Chemie der Universität Mainz.
⊗ Abstract published in *Advance ACS Abstracts,* October 1, 1996.

S0024-9297(96)00835-2 CCC: $12.00

III includes a thorough description and evaluation of the results in the three regimes, namely, homogeneous, in the vicinity of phase separation, and the two-phase region. Finally, the main conclusions are summarized in section IV.

II. Experimental Section

Materials. Samples of PVME with a reasonably low polydispersity index M_w/M_n were obtained by continuous polymer fractionation (CPF).[10] The original material was the commercial Lutonal M40, from BASF. The specific sample used in the present work was a PVME with $M_n = 64$ kg/mol, $M_w = 87$ kg/mol, and $M_w/M_n = 1.35$. Nearly monodisperse PS with $M_w = 92$ kg/mol and $M_w/M_n = 1.03$ was obtained from Pressure Chemical Co., Pittsburgh, PA. Both PS and PVME are well entangled, since their entanglement molecular weights, determined from their plateau moduli,[12] are $M_{e,PS} = 18\,000$ and $M_{e,PVME} = 6000$, respectively. PVME is known to be sensitive to chemical degradation, reflected by a yellowish color, which is representative of oxidation taking place.[13] In order to exclude the possibility of any effects of degradation on the reported results, we have carried out fractionation and rheological measurements; the latter confirmed that the molecular weight and polydispersity, as well as the viscoelastic properties, remained unchanged throughout the course of this work. Moreover, it is noted that the color of PVME remained unchanged; it was off-white with a slight yellow appearance, as already reported elsewhere.[10]

Blends of various compositions were prepared from ternary solutions of PS and PVME in toluene. Firstly, the solvent was allowed to evaporate at room temperature for about 3 days. Then the samples were dried under vacuum for 12 h at 40 °C and for about 2 days at 70 °C, until the solvent was completely removed, as judged by the constant weight and constant T_g of the sample. Since PVME is known to be hygroscopic, it was ascertained that the blends must remain free of moisture, to avoid any undesirable effects on the phase behavior.

Methods. The phase diagram was obtained by utilizing turbidimetry. A laser beam of intensity I_0 (5 mW He−Ne laser at 632.8 nm) was sent through the sample, and the transmitted intensity (at 0° angle), I, was measured as a function of temperature, T, upon heating, starting from low temperatures in the homogeneous regime.

The viscoelastic properties of the blends were measured by shear rheology. Two controlled stress rheometers were used: a Rheometric Scientific SR-200 and a Carri-Med CSL-500. Various geometries were chosen, namely, parallel plates with diameter 25 or 8 mm and cone-and-plate with diameter 20 mm and an angle of 1° (Peltier element) or 2° (high temperature element). Temperature control was achieved either by electrically heated plates or by the Peltier element. In each case the accuracy was ±0.1 °C. The temperature varied from 0 to 135 °C, covering the whole range of blend behavior, from homogeneous to phase separated. The CSL-500 rheometer with the cone-and-plate geometries was utilized for the measurements in the well-homogeneous regime, while the SR-200 rheometer was employed for the measurements in the pretransitional and phase-separated states. All measurements were carried out under N_2 atmosphere to prevent any degradation or absorption of moisture. The following small amplitude oscillatory shear measurements were carried out for each blend at a fixed composition: (i) dynamic time sweeps at a given temperature and frequency (from 0.1 to 1 rad/s), in order to obtain steady state and thus ensure that measurements were performed under "dynamic equilibrium" conditions; (ii) dynamic stress sweeps at a given temperature and frequency (0.1 rad/s to 100 rad/s), to determine the limits of linear viscoelasticity; (iii) isochronal dynamic temperature ramps (at a given low frequency) by increasing the temperature from the homogeneous to the phase-separated regime, at a certain stress and heating rate, in order to determine the effects of temperature (and in particular phase separation) on the linear viscoelastic properties of the blend; and (iv) isothermal dynamic frequency sweeps from 0.01 to 100 rad/s at a given stress, in order to determine the behavior of the storage (G') and loss (G'') moduli in the homogeneous, transitional, and two-phase regimes. Further, in the homogeneous regime, steady shear measurements, namely creep experiments, were carried out in order to accurately determine the zero-shear viscosity, η_0, and establish mixing rules.

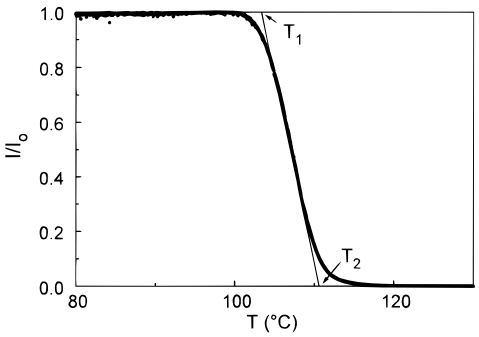

Figure 1. Intensity (I) of the transmitted laser beam (normalized to the incident intensity, I_0) as a function of temperature for 60/40 PS/PVME at a heating rate of 0.1 °C/min.

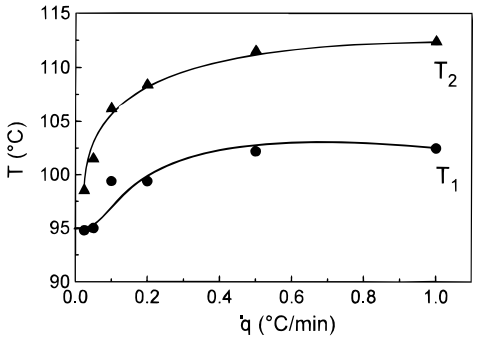

Figure 2. Dependence of demixing temperatures T_1 (●) and T_2 (▲) on the rate of heating for a 50/50 PS/PVME blend. Lines are drawn to guide the eye.

The glass transition temperatures of the PS/PVME blends of various compositions, including the pure components, were measured with a differential scanning calorimeter (DSC), from Polymer Laboratories, model PL-DSC.

III. Results and Discussion

Determination of the Phase Diagram. For finite heating rate, $\dot{q}$, the turbidity of the blend develops in a finite temperature range which can reach up to 10 °C. This behavior is likely due to the high viscosity of the blends (mainly attributed to the "hard" PS component), which slows down the phase separation. For a given heating rate, the temperature extrapolated to the onset of turbidity, T_1, is taken as the cloud point temperature, T_{cp}. This is shown in Figure 1, which depicts a typical example of turbidimetric determination of T_{cp} for a 60/40 PS/PVME blend (60% per weight in PS), with a heating rate of 0.1 °C/min. The extrapolated temperature of total darkness, T_2, is also indicated in Figure 1. T_1 can be reproduced within ±1 °C for this heating rate. The effects of $\dot{q}$ for a range of values from 0.05 to 1 °C/min on T_1 and T_2 are illustrated in Figure 2. It is apparent that neither $T_{cp}(\dot{q})$ nor $T_{cp}(\sqrt{\dot{q}})$ (not shown here), yield a linear dependence. For this reason the data for 0.1 °C/min are taken for the subsequent considerations in spite of the fact that T_{cp} still decreases measurably with a reduction of $\dot{q}$. According to Figure 2, the errors introduced by this procedure should remain below 5 °C. The thus obtained phase diagram is depicted in Figure 3; both the T_1 curve (cloud point curve) and the T_2 points are included in this graph. The error bar at 70 wt % PS is indicative of the reproducibility of the cloud points. From the experience that the critical composition is slightly shifted out of the extreme

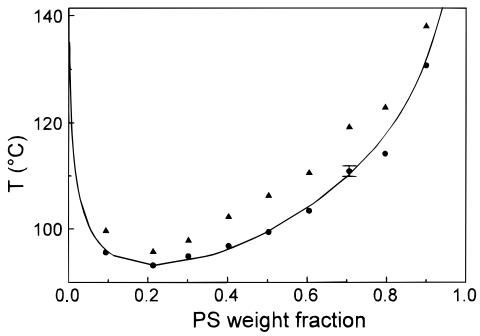

Figure 3. Cloud point curve of PS/PVME (T_1 was taken as the cloud point temperature, T_{cp}) obtained with a heating rate of 0.1 °C/min. The error bar is shown at the 70% PS T_1 data point. The solid line is the calculated curve with the χ of eq 2: T_1, ●; T_2, ▲.

of the cloud point curve toward the component with the larger molecular polydispersity,[14] it can be inferred that the critical composition is slightly less than 20 wt % in PS. It is further noted that in the phase-separated envelope the samples have the expected cloudy appearance.

For the calculation of the cloud point curve shown in Figure 3, on the basis of the equality of the chemical potentials, it is assumed for simplicity that both polymers are uniform. The Flory-Huggins integral interaction parameter, χ, of eq 1, is appropriately adjusted as a function of blend composition (φ) and temperature (T, in K) in eq 2, using the following values for the segmental volume and the number of segments of the components: $V_{segment} = 100$ cm^3/mol, $N_{PS} = 878$, $N_{PVME} = 817$.

$$\frac{\overline{\Delta G}}{RT} = \frac{1}{N_{PS}}\varphi_{PS} \ln \varphi_{PS} + \frac{1}{N_{PVME}}\varphi_{PVME} \ln \varphi_{PVME} + \chi\varphi_{PS}\varphi_{PVME} \quad (1)$$

where φ_{PS} and φ_{PVME} are the volume fractions of PS and PVME, respectively, and[15]

$$\chi = -4.0953 \times 10^{-3} + \frac{0.03164 - \frac{10}{T}}{1 - 0.36\varphi_{PVME}} \quad (2)$$

Shear Rheology. Homogeneous Regime. Zero shear viscosities, η_0, are determined from creep measurements according to[12]

$$\gamma(t)/\sigma_0 = J_e^0 + t/\eta_0 \quad (3)$$

where t is the time (in s), $\gamma(t)$ the shear strain (%), σ_0 the shear stress (in dyn/cm^2), and J_e^0 the steady state shear compliance (in cm^2/dyn).

The dependence of the viscosity on temperature can be described by the WLF equation:[12]

$$\log \frac{\eta_{0,T}}{\eta_{0,T_0}} = \frac{c_1(T - T_0)}{c_2 + (T - T_0)} \quad (4)$$

The values for the parameters c_1 and c_2 of this relation, obtained from fitting of the η_0 data with the above equation, are given for different blend compositions at the reference temperature $T_0 = 70$ °C in Table 1.

The dependence of η_0, on blend composition is measured at 70 °C, where the components are still completely miscible. Blends with volume fractions of PS (φ_{PS}) ≥ 0.86 have a glass transition temperature (T_g) above 70 °C and are therefore not studied. The viscosities of the blends with $0 < \varphi_{PS} \leq 0.86$ are described within experimental error by the simple relation:[16]

Table 1. Parameters of the WLF Equation for Homogeneous PS/PVME Blends (Reference Temperature $T_0 = 70$ °C)

φ_{PS}	c_1	c_2(K)	φ_{PS}	c_1	c_2(K)
0	7.86	218.4	0.43	10.89	210.7
0.17	6.86	153.7	0.67	16.07	232.9
0.25	13.24	304.8	0.77	11.95	155.3
0.33	9.79	203.4	0.86	8.37	74.1

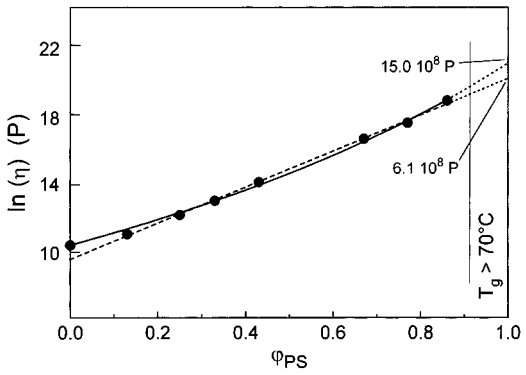

Figure 4. Dependence of the zero-shear viscosity (●) on blend composition at 70 °C: solid line, fitting with eq 6; dashed line, fitting with eq 5.

$$\ln \eta = \varphi_{PVME} \ln \eta_{PVME}^{fit(5)} + \varphi_{PS} \ln \eta_{PS}^{fit(5)} \quad (5)$$

where the superscripts "fit" serve as a reminder that these viscosities are fitting values only. The thus obtained values are 1.58×10^4 P for $\eta_{PVME}^{fit(5)}$ instead of the measured value of 3.63×10^4 P and 6.1×10^8 P for $\eta_{PS}^{fit(5)}$. Figure 4 depicts the viscosity as a function of composition at 70 °C and the corresponding best fit line (dashed) based on eq (5); because of the pronounced deviation of the data point for pure PVME, a new approach[17] for the description of the viscosities of mixtures is tested. It adds a term to the above relation, taking account for the differences in the molecular shape of the components, as follows:

$$\ln \eta = \varphi_{PVME} \ln \eta_{PVME} + \varphi_{PS} \ln \eta_{PS}^{fit(6)} + \ln\left(\frac{\eta_{PS}^{fit(6)}}{\eta_{PVME}}\right)\left(\frac{\gamma\varphi_{PS}\varphi_{PVME}}{1 + \gamma\varphi_{PS}}\right) \quad (6)$$

where γ is a geometric factor, measuring the difference between volume and surface fractions. In the present case, γ and the viscosity of the hypothetical "supercooled" melt of polystyrene, $\eta_{PS}^{fit(6)}$, are fitted according to the above relation on the basis of the measured viscosity of the pure PVME ($\eta_{PVME} = 3.63 \times 10^4$ P) and the measured viscosities of the blends. The results are $\gamma = -0.35$ and $\eta_{PS}^{fit(6)} = 1.5 \times 10^9$ P. The parameter γ can also be obtained by the group contribution method using values tabulated by Bondi.[18] It is calculated from the van der Waals volumes and the van der Waals surfaces of the two polymeric components of the blend, by the following equation:

$$\gamma_B = \frac{N_F}{N_V} - 1 \quad (7)$$

where the subscript B refers to Bondi's method, $N_F = F_{PS}/F_{PVME}$ and $N_V = V_{PS}/V_{PVME}$, with F_A being the van

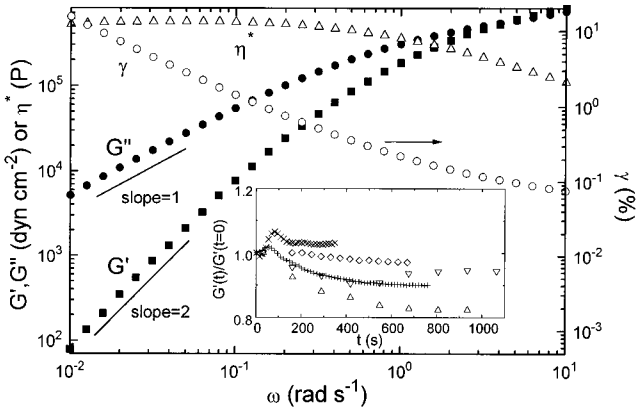

Figure 5. Typical frequency sweep of a 40/60 PS/PVME blend in the homogeneous region (T = 90 °C); the applied stress amplitude is 800 dyn/cm^2: G', ■; G'', ●; η^*, △; γ, ○. Inset: dynamic time sweeps of G' (normalized to that at time $t = 0$) with $\omega = 0.05$ rad/s and the same stress, at various temperatures in the one-phase and two-phase regions: 90 °C, △; 93 °C, ▽; 100 °C, ◇; 105 °C, +; 110 °C, X.

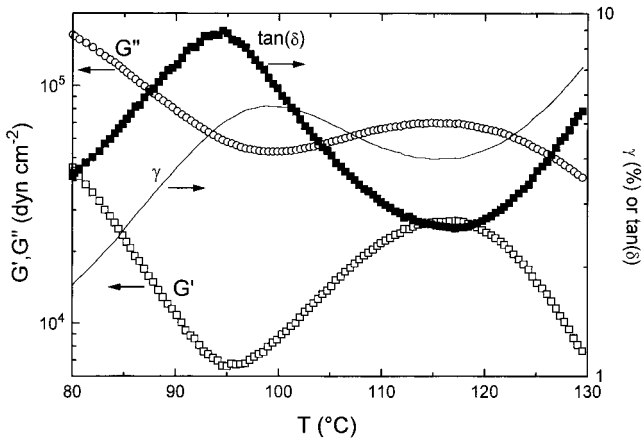

Figure 6. Isochronal (ω = 0.1 rad/s) dynamic temperature ramp of 40/60 PS/PVME for an applied stress amplitude of 1000 dyn/cm^2 and a heating rate of 0.1 °C/min: G', □; G'', ○; tan δ, ■; γ, −.

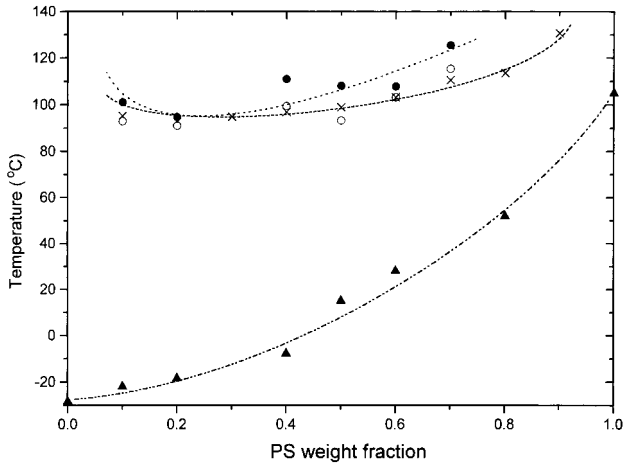

Figure 7. Phase diagram of a PS/PVME blend as determined by shear rheology: T_{rheo}, ○; spinodal temperature, T_s, ●. Cloud points determined from turbidity (T_1) are also depicted (X). The dashed and dotted lines are drawn to guide the eye. Also depicted are the average T_g's of the blend (▲), with a line to guide the eye.

der Waals surface and V_A the corresponding volume of component A.[18] For the PS/PVME blend of this work, the method yields $\gamma_B = -0.15$. In view of the fact that the information on surfaces and volumes stems from thermodynamic instead of rheological sources and that polymers instead of low molecular weight substances are investigated here, the agreement may be considered reasonable. From the above discussion it is concluded that eq 6, a mixing rule established for low molecular weight compounds, can also be applied to the blend viscosity in the homogeneous regime as function of composition rather well.

A typical dynamic frequency sweep is depicted in Figure 5, for a well-homogeneous 40/60 PS/PVME blend at 90 °C. At low frequencies in the terminal regime, the expected[12] $G' \sim \omega^2$ and $G'' \sim \omega^1$ scaling laws are obtained. Note that the maximum strain, γ, of 13% is within the limits of linear viscoelasticity. Further, the inset of Figure 5 confirms that the dynamic measurements at various temperatures in the homogeneous and phase-separated region were carried out under steady state conditions.

Pretransitional Regime. As the phase separation temperature is approached for a given composition, the viscoelastic properties of the blend change substantially. A typical example illustrating the effects of phase separation is depicted in the temperature ramps of Figure 6, for the 40/60 blend at a heating rate of 0.1 °C/min and frequency of 0.1 rad/s. At low temperatures in the homogeneous regime, an increase of temperature results in a decrease of G' due to mobility effects associated with an increased distance from the T_g of the blend. As the temperature increases further, the phase boundary is approached; the latter is associated with the thermodynamic slowing down of the thermal decay rate of concentration fluctuations, which increase in amplitude when the distance from the spinodal temperature, T_s, is decreased. In other words, in the vicinity of phase separation, there is a competition between mobility and thermodynamics.[5] The net result is an increase of G' due to the latter forces, i.e. the formation of dynamic domains rich in the hard PS component of the blend. From Figure 6 it is apparent that at a temperature of about 95 °C, these forces dominate, up to about 115 °C. Above that temperature, mobility forces control again the viscoelastic behavior of the phase-separated (based on Figure 3) blend. We argue that the temperature region between 95 and 115 °C, which is characterized by the dominance of the thermodynamic forces, is associated with the phase separation. In particular, we assign the inflection point in the G' vs T curve in this temperature region in the specific example of Figure 6 (the maximum of dG'/dT occurs at 106.5 °C) to the (rheological) phase separation curve. This assignment is empirical and not based on specific physical grounds. Nevertheless, it accounts for an apparent concentration fluctuations-induced enhancement in G' in the one-phase regime; the latter results in a thermorheologically complex behavior, in the pretransitional regime, as will be discussed below. The thus determined rheological demixing temperatures, T_{rheo}, are in very good agreement with those obtained from turbidity, T_{cp}, as seen in Figure 7. It should be emphasized that the rheological demixing temperatures are all determined from dynamic temperature ramps carried out at frequencies between 0.1 and 1 rad/s and heating rates between 0.07 and 1 °C/min. In all cases the estimated demixing temperatures are nearly independent of the heating rate, in agreement with the relevant turbidity investigations (Figure 2). Figure 7 also depicts the average T_g of the blends of different compositions, as measured by DSC. For each case, one single broad T_g is detected.

Similar behavior is also exhibited by the other viscoelastic material functions, as seen in Figure 6. In

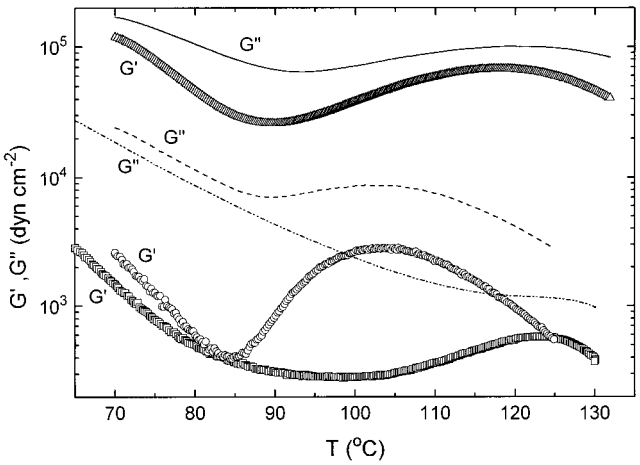

Figure 8. Temperature dependence of storage moduli (G') and loss moduli (G'') at various PS/PVME blend compositions: 10/90, G' (□) and G'' (− - - −); 20/80, G' (○) and G'' (- - -); 40/60, G' (△) and G'' (−). All measurements refer to frequency ω = 0.5 rad/s and a heating rate of 0.5 °C/min.

particular, G'' is also sensitive to the above mentioned interplay of mobility and thermodynamics, but to a much lesser extent; this is in agreement with similar behavior observed in diblock copolymers[8] and also predicted by a mean field theory,[19,20] which will be discussed below. The higher sensitivity of G' is attributed to the fact that the stress induced to the system by the concentration fluctuations is mostly of elastic origin. Also, if one thinks in terms of simple mechanical models describing the terminal relaxation, such as the Maxwell model, the elastic component responds first and more sensitively to a given deformation, compared to the viscous contribution. Besides the small upturn in G'', compared to G', it is also noted in Figure 6 that the upturn in G'' occurs roughly 4 °C above the G' minimum; in other words, the viscous dissipation part of the blend responds with some retardation to the thermodynamic effects of phase separation. This retardation is apparently related to the phase lag between the elastic and viscous components of the stress, as well as the above mentioned mechanical analogy. The strain varies within the limits of linear viscoelasticity; its behavior is easily understood in terms of its definition $\gamma = \sigma/G^*$, with σ being the imposed stress amplitude and G* the complex modulus. Finally, the trend of the tan δ curve stems from those of G' and G''.

A few remarks concerning the magnitude of the upturn in viscoelastic properties (in G′ for example) are in order. The interpretation of this upturn, as attributed to the formation of dynamic regimes rich in the high modulus PS component, induced by the enhanced concentration fluctuations near the phase boundary, relates to the dynamic asymmetry (T_g-contrast) of the two blend components. It is noted that in LCST systems with nearly no T_g-contrast, there is effectively no upturn in G' as the temperature approaches the phase boundary; only a clear reduction of slope is observed.[21] Moreover, Figure 8 depicts the temperature dependence of the elastic muduli of PS/PVME at various compositions, namely, 10/90, 20/80 (critical), and 40/60. From this figure the effects of changing composition on the shape of the temperature-dependent moduli curves are apparent; they can be explained by the fact that changing composition changes the distance of the effective blend T_g from the T_g's of the individual components,[11] which in turn is responsible for the viscoelastic behavior of the blends. It is also evident from this figure that not only the magnitude of the upturn, but also the

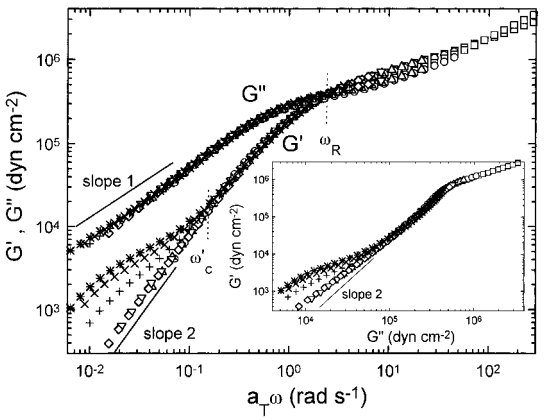

Figure 9. Master curves of G' and G'' for the 70/30 PS/PVME blend as a function of shifted frequency $\alpha_T\omega$, where α_T is the temperature shift factor. The reference temperature is 90 °C. A failure of the time-temperature superposition principle is observed at low frequencies. The two solid lines have slopes 2 (G') and 1 (G''). Inset: log−log representation of shear-moduli G' versus G''. The solid line represents a slope of 2. The frequencies ω_R and ω_c' correspond to the longest relaxation time and the onset of thermorheological complexity, respectively. Symbols: 90 °C, □; 95 °C, ○; 100 °C, △; 105 °C, ▽; 110 °C, ◇; 120 °C, +; 130 °C, X; 135 °C, ∗.

temperature range over which the upturn takes place is strongly dependent on this dynamic asymmetry. Of course, it should be kept in mind that, for the temperatures corresponding to phase-separated systems, the viscoelastic properties are time-dependent due to the coarsening of the phase-separated structure. Nevertheless, the demixing temperature, T_{rheo}, can always be determined from the upturn in G', as discussed before.

Returning to the issue of thermorheological complexity, the isothermal frequency sweeps for a given composition are all plotted together in the form of master curves, obtained by shifting along the frequency axis. A representative example is illustrated in Figure 9, for G' and G'' of the 70/30 blend. At high frequencies the entanglement plateau region is reached, while at lower frequencies the system flows in the terminal regime. It is apparent that for the temperatures in the homogeneous regime (up to 110 °C; see the phase diagram of Figure 7) the principle of time-temperature superposition (TTS) holds for both G' and G''. However, the data in the two-phase region do not superpose the homogeneous ones. This observation is also evident in the inset of Figure 9 which depicts the log G' vs log G'' plot; such a plot has been suggested to be more sensitive than TTS to phase transitions.[22−24] More specifically, as the temperature increases well into the phase-separated regime, an apparent deviation from the terminal slope is observed in the G' curve (enhancement of elasticity), which is actually responsible for the thermorheological complexity. This "enhanced elasticity" is undoubtedly related to the morphology of the phase-separated blend. It persists only over a small range of low frequencies, and it does not correspond to a terminal solid-like relaxation of the system; at even lower frequencies the system will eventually flow, reaching the terminal slope of nearly 2. Similar observations hold for the behavior of G'' as well, but with much reduced sensitivity.

An important question, addressed before (Figure 6), is whether the enhanced concentration fluctuations in the homogeneous regime near T_{rheo} produce any increase in G' that leads to detectable deviation from TTS, as for instance is observed in the case of block copolymers.[9] To address this issue, it is necessary to perform the frequency sweeps with very small temperature steps,

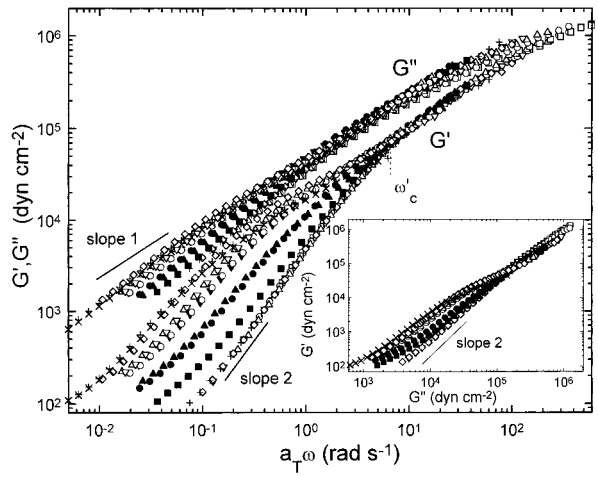

Figure 10. Master curves of G' and G'' for 20/80 PS/PVME with a reference temperature of 78 °C. The two solid lines have slopes 2 (G') and 1 (G''). Inset: representation of the thermorheological behavior as log G' versus log G''. The solid line denotes a slope of 2. Symbols: 60 °C, □; 65 °C, ○; 70 °C, △; 75 °C, ▽; 78 °C, ◇; 81 °C, +; 90 °C, ■; 93 °C, ●; 95 °C, ▲; 98 °C, ▼; 100 °C, ○; 102 °C, △; 105 °C, ▽; 110 °C, ◇.

as the phase boundary is approached. Results from such measurements are shown in Figure 10 for the 20/80 blend. It is indeed clear that TTS fails while in the homogeneous regime, near the phase boundary. This result confirms the qualitative similarities with block copolymers,[9] although in the latter case the effects are apparently stronger.[9,19,20] In the inset of Figure 10 the storage modulus is plotted against the loss modulus in a log−log representation. The same remarks hold as for Figure 9. Furthermore, the critical frequency, ω_c', corresponding to the onset of thermorheological complexity (Figures 9 and 10) is assessed with respect to its dependence on the blend composition. The corresponding characteristic time, $\tau_c = 1/\omega_c'$, is within the spectrum of terminal relaxation, and in that respect, it is considered proportional to the terminal relaxation time of the blend τ_R. From the experimental data, τ_c increases as the PS content of the blend increases, and this can be explained in view of the above argument on PS-rich domains. The fact that $\tau_c \gg \tau_R$ suggests that the failure of TTS is associated with time scales much larger than the ones corresponding to the motion of one chain; such time scales could relate to "collective" motion of several chains, e.g. motion of pseudodomains rich in PS, formed as a result of phase separation.

Having established the phenomenology of the effects observed in the transitional regime of phase separation, we now turn to their quantitative evaluation. To do so, we consider the theoretical approach of Ajji and Choplin.[19] These authors have extended the earlier theoretical treatment of Fredrickson and Larson for block copolymer melts near the order−disorder transition[20] to the case of homopolymer blends. Mean-field theory has been employed to derive the critical contribution to the shear stress for near-critical polymer mixtures; after integration over wavevector space, the following expressions can be obtained for the dynamic storage and loss moduli, respectively:

$$G'(\omega) = \frac{k_B T \omega^2}{15\pi^2}\int_0^{k_c} \frac{k^6 S_0^2(k)}{\omega^2 4_\omega^{-2}(k)}\left[\frac{\partial S_0^{-1}(k)}{\partial k^2}\right]^2 \mathrm{d}k \qquad (8)$$

$$G''(\omega) = \frac{2k_B T \omega}{15\pi^2}\int_0^{k_c} \frac{k^6 S_0^2(k)\bar{\omega}(k)}{\omega^2 4\bar{\omega}^2(k)}\left[\frac{\partial S_0^{-1}(k)}{\partial k^2}\right]^2 \mathrm{d}k \qquad (9)$$

where $\bar{\omega}(k) = k^2 S_0^{-1}(k)\lambda(k)$, $S_0(k)$ is the static structure factor, and $\lambda(k)$ the Onsager coefficient, with k the wavevector. These equations have been applied for the case of binary polymer blends by utilizing the de Gennes mean field structure factor,[26]

$$\frac{1}{S_0(k)} = \frac{1}{\phi N_1 g_1(k)} + \frac{1}{(1-\phi)N_2 g_2(k)} - 2\chi \qquad (10)$$

with N_i being the number of statistical segments, $g_i(k)$ the Debye function, and the expression for the Onsager coefficient proposed by Binder:[25]

$$\frac{1}{\lambda(k)} = \frac{1}{\phi b_1^2 W_1 g_1(k)} + \frac{1}{(1-\phi) b_2^2 W_2 g_2(k)} \qquad (11)$$

In eq 11, b_i is the statistical segment length for species i and W_i its rate of reorientation:

$$W_i = 3\pi k_B T/\zeta_i \qquad (12)$$

with ζ_i being the monomeric friction coefficient. For the terminal one-phase region near the critical point, these expressions become

$$G'(\omega) = \frac{k_B T \omega^2}{1920\pi}\left[\frac{1}{3}\left\{\frac{R_{g_1}^2}{\phi N_1} + \frac{R_{g_2}^2}{(1-\phi)N_2}\right\}\right]^{1/2}\left[\frac{1}{\phi b_1^2 W_1} + \frac{1}{(1-\phi) b_2^2 W_2}\right][2(\chi_s - \chi)]^{-5/2} \qquad (13)$$

$$G''(\omega) = \frac{k_B T \omega}{240\pi}\left[\frac{1}{3}\left\{\frac{R_{g_1}^2}{\phi N_1} + \frac{R_{g_2}^2}{(1-\phi)N_2}\right\}\right]^{1/2}\left[\frac{1}{\phi b_1^2 W_1} + \frac{1}{(1-\phi) b_2^2 W_2}\right]^2 [2(\chi_s - \chi)]^{-1/2} \qquad (14)$$

where χ_s designates the interaction parameter at the spinodal, i.e. when $S_0^{-1}(0) = 0$, and R_{g_i} is the radius of gyration of species i. By properly manipulating the above expressions (13 and 14), one can calculate the ratio

$$\frac{G'(\omega)}{[G''(\omega)]^2} = \frac{30\pi}{k_B T}\left\{\frac{b_1^2}{36\phi} + \frac{b_2^2}{36(1-\phi)}\right\}^{3/2}(\chi_s - \chi)^{-3/2} \qquad (15)$$

The interesting feature of eq 15 is that the monomeric friction coefficients are eliminated; this result is considered important, since the segmental dynamics of multicomponent systems, which is associated with the monomeric friction, is not fully understood yet (see for example ref 27). Assuming that the interaction parameter is given by $\chi = A + B/T$, a linear dependence is predicted of $\{[G''(\omega)]^2/(G'(\omega)T)\}^{2/3}$ versus $1/T$, leading to an intercept with the $1/T$ axis denoting the spinodal temperature, T_s. Indeed, Figures 11 and 12 show typical representations of the data for the 20/80 and the 40/60 blends, respectively, where a linear range is observed in the data in the pretransitional regime. The corresponding line gives an estimate of the spinodal temperature, indicated by an arrow. Deviations are observed at both the high and the low temperature side in these figures. This is due to the fact that the theory has been developed for the one-phase region but in close proximity to the critical point (for large correlation lengths), where the concentration fluctuations contribu-

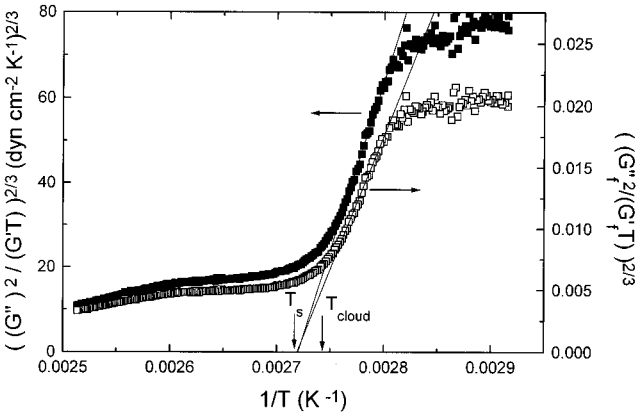

Figure 11. Quantitative evaluation (■) of the viscoelastic behavior of the 20/80 PS/PVME blend near the phase separation and determination of the spinodal temperature. Vertical arrows indicate spinodal and cloud points. Also shown (□) is the determination of spinodal temperature from the estimated excess fluctuation-induced shear stress, as described in the text.

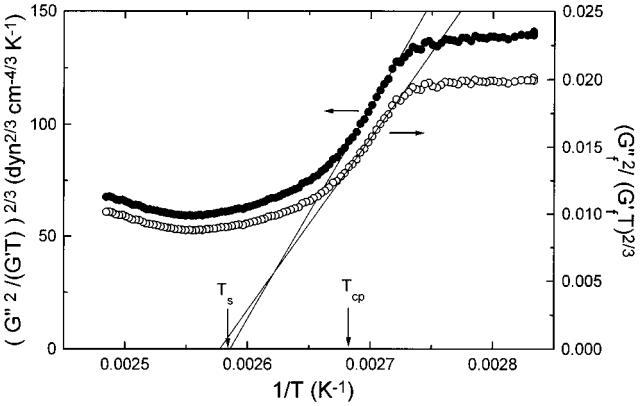

Figure 12. Quantitative evaluation (●) of the viscoelastic behavior of the 40/60 PS/PVME blend near the phase separation and determination of the spinodal temperature. Vertical arrows indicate spinodal and cloud points. Also shown (○) is the determination of spinodal temperature from the estimated excess fluctuation-induced shear stress, as described in the text.

tions to G' and G'' are dominant; thus, it applies for low enough temperatures in the well-homogeneous state, not for high temperatures in the two-phase region. It is also noted that the selection of the linear range is crucial for the determination of T_s and in the present case involves an error of about ±2 °C. Referring to the above analysis, it is important to point out that the theoretical approach of Fredrickson and Larson[20] accounts for the excess shear stress induced by the enhanced concentration fluctuations in the pretransitional region in the case of blends. On the other hand, the rheological measurements record the global response of the system, i.e. both flow- and thermodynamics-induced contributions to shear stress. To account for the latter, we consider as "background" (G'_b or G''_b) the stress at low temperatures in the homogeneous regime, where no thermodynamic effects interfere whatsoever. By assuming that its functional dependence on temperature does not change (Figures 6, 8), we can extrapolate the modulus to higher temperatures and then obtain an estimate of the excess shear stress from the ratio $G'_f = G'/G'_b$ or $G''_f = G''/G''_b$ at different temperatures, where the subscript f refers to fluctuations. The values G'_f and G''_f reflect the fluctuation-induced contribution to the stress (under the further assumption that friction in both "total" and "background" moduli has the same temperature dependence) and are subsequently used in the analysis to determine T_s. The results are shown in Figures 11 and 12 and are truly satisfactory (same T_s within 2 °C), suggesting that a standard "global" rheological measurement can indeed be accounted for with this mean field theory and used to determine the spinodal temperature. It is noted that the theoretical approach presented here applies very well for this LCST system, although it has been originally developed for upper critical solution temperature (UCST) systems. Its applicability for UCST systems is currently under investigation,[28] although it is recognized that the effects of phase behavior are incorporated in the χ parameter.

The thus determined spinodal temperatures are depicted in Figure 7. The critical composition is estimated to be 20/80 PS/PVME, where $T_s \approx T_{rheo}$; this is in agreement with the turbidimetric data of Figure 3, for $T_1 \approx T_2$. However, it is noted that the T_2 temperature, although possibly related somehow to T_s, may not necessarily be equal to T_s; nevertheless, the rheological T_s and turbidimetric T_2 data seem to be in reasonable agreement (as judged from Figures 3 and 7). Therefore, we argue on the basis of Figure 7 that a single shear rheological measurement is adequate in providing complete information on the phase diagram of a binary polymer blend.[29] It is noted that, by modifying eq 15, the correlation length (ξ) of blends can be estimated from the ratio $G'/(G'')^2$ as a function of temperature. The thus determined value of ξ increases significantly as the phase separation temperature is approached, in agreement with theoretical predictions and other data.[19] As a further remark, the straight lines in Figures 11 and 12 represent evidence of the validity of the idea that the thermorheological complexity in the pretransitional regime is due to large concentration fluctuations. They also show that the theory conforms to the experimental observations concerning (i) the much weaker temperature dependence (and thus sensitivity) of G'' compared to G' and (ii) the reduced sensitivity of viscoelastic properties of blends to phase separation, when compared to block copolymers at the same distance from the phase boundary (the latter, only indirectly).

Phase-Separated Regime. In this regime, the underlying characteristic is the deviation from TTS, associated with the enhanced moduli (with respect to the terminal slopes). It is clear that the phase morphology[30] is the key parameter responsible for the observed thermorheological complexity, as is evident in Figures 9 and 10. The appearance of the region of enhanced moduli, which is mostly noticeable at higher PS concentrations, results in a splitting of the terminal relaxation into two processes. Whereas the slow process should be related to the relaxation of the phase-separated blend (which is of structural origin), as observed in other systems as well,[31] the nature of the faster process is not clear; it is apparently related to the higher concentration of PS-rich domains, which are redistributed in the two-phase system, before the latter eventually flows. Moreover, as is clear from Figures 9 and 10, and was already mentioned, the transient plateau is followed by the terminal relaxation with $G' \sim \omega^2$ at very low frequencies. This observation clears the situation, since earlier investigations discussed the apparent beginning of the enhanced elasticity region in terms of a different power law dependence of G'.[5]

This complex viscoelastic behavior in the two-phase regime is quantitatively analyzed by utilizing a theoretical approach for describing the rheology of emulsions of incompressible viscoelastic fluids. This approach was

first considered in the description of the rheological behavior of incompatible polymer blends in the melt,[31] where a general observation was the substantial increase of elasticity at low frequencies, in the terminal regime. It was recognized that this enhancement could be described by constitutive equations for emulsions of two Newtonian liquids[32] or emulsions of two viscoelastic fluids;[33] the latter could better account for the high-frequency behavior as well, and thus it was used for the case of immiscible polymer blends. In this work we adopt essentially this approach in order to quantify the rheological characteristics of phase-separated PS/PVME blends. These systems are considered as emulsions of viscoelastic incompressible materials, where the "suspended" particles forming the dispersed phase are assumed to be nearly spherical and their deformation remains small, i.e. within the limits of linear viscoelasticity. The pronounced elasticity at low frequencies is actually attributed to the interfacial tension. Under the further assumption that the interfacial tension between the matrix and the dispersed phase is independent of local shear and variation of interfacial area and that the dispersed spherical droplets are nearly monodisperse, the model[29] leads to the following expression for the complex modulus of the two-phase mixture (emulsion), $G^*(\omega)$:

$$G^*(\omega) = G_m^*(\omega)\frac{1 + 3\phi H(\omega)}{1 - 2\phi H(\omega)} \tag{16}$$

$$H(\omega) = [4(\alpha/R)(2G_m^*(\omega) + 5G_i^*(\omega)) + (G_i^*(\omega) - G_m^*(\omega))(16G_m^*(\omega) + 19G_i^*(\omega))]/[40(\alpha/R)(G_m^*(\omega) + G_i^*(\omega)) + (2G_i^*(\omega) + 3G_m^*(\omega))(16G_m^*(\omega) + 19G_i^*(\omega))] \tag{17}$$

where the subscripts m and i refer to the matrix and dispersed phase (inclusions), respectively, α is the interfacial tension, and φ is the volume fraction of the inclusions of size R. It can be easily shown that this model can be generalized to the case of polydisperse inclusions and also reduce to a number of useful simpler models.[31] However, here we simply employ the general formulation for monodisperse inclusions, described by the above equations. Further, it is clear from eqs 16 and 17 that the modulus of the emulsion can be estimated (and thus compared against experimental data) only if the corresponding moduli of the two constituents are known. Due to the phase diagram involved here, the phase-separated blend in the temperature range of our measurements will never actually consist of pure PS and pure PVME domains; instead, it consists of PS-rich and PVME-rich domains, with composition determined by the tie lines of the phase diagram, and thus we interpret the inclusions and matrix of the emulsion as these domains into which a phase-separated blend of a given concentration can be decomposed, on the basis of its phase diagram (Figure 7). More specifically, we examine the 40/60 PS/PVME blend at 110 °C. This can be thought of as inclusions of PS-rich spherical domains of constant size with concentration 60% PS (60/40 PS/PVME) dispersed in a matrix of PVME-rich domains with concentration 10% PS (10/90 PS/PVME). Application of the above model, with one only adjustable parameter, namely the ratio (α/R), produces the results depicted in Figure 13. The model predictions depend on (α/R) and are in qualitative agreement with the experimental data, especially with respect to the observed change of slope at low frequencies; the latter is more apparent for the case $(\alpha/R) = 10^3$ dyn/cm^2. Further, for a value of $(\alpha/R) = 0$ dyn/cm^2, which corresponds to a dispersion of incompressible Hookean inclusions in an incompressible Hookean matrix,[31] the quantitative agreement is very reasonable, especially at low frequencies; larger deviations (by approximately a factor of 2) occur at higher frequencies. Once again, the model results show higher sensitivity in the elastic modulus. This is considered satisfactory, given the rather rough assumptions concerning the dispersed phase. Another limitation related to the assumption of spherical monodisperse droplets has to do with the fact that due to experimental conditions (referring to Figure 7), the temperature studied is near the phase boundary.

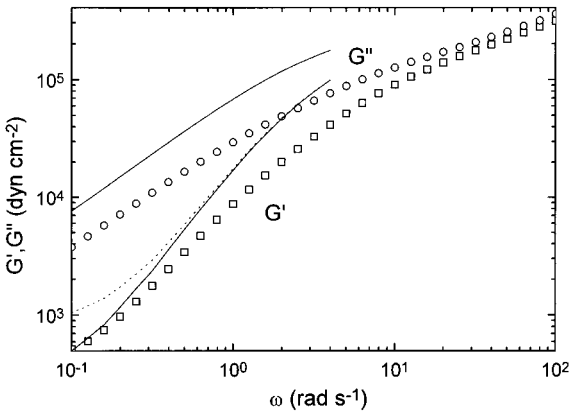

Figure 13. Evaluation of the rheology of the phase-separated 40/60 PS/PVME blend at 110 °C: experimental data, G' (□) and G'' (○); solid lines, emulsion model predictions (eqs 16 and 17) for $(\alpha/R) = 0$ dyn/cm^2; dashed lines, model predictions for $(\alpha/R) = 10^3$ dyn/cm^2, $T_{cp} = 99.5$ °C. For G'', the two theoretical curves are indistinguishable.

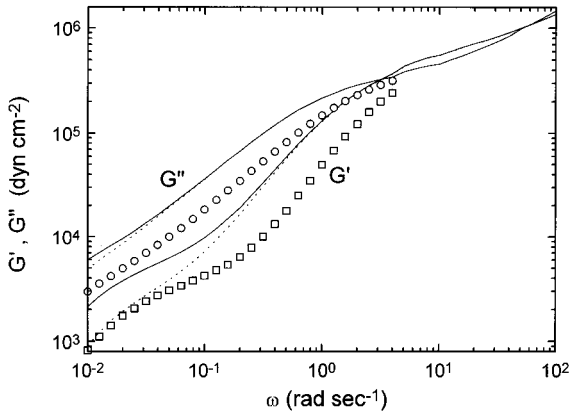

Figure 14. Evaluation of the rheology of the phase-separated 60/40 PS/PVME blend at 130 °C: experimental data, G' (□) and G'' (○); solid lines, emulsion model predictions (eqs 16 and 17) for $(\alpha/R) = 10^4$ dyn/cm^2; dashed lines, model predictions for $(\alpha/R) = 0$ dyn/cm^2, $T_{cp} = 103$ °C.

The situation is more interesting in the case of the 60/40 PS/PVME blend at 130 °C, which can be considered as consisting of a 70/30 PS/PVME matrix and pure PVME inclusions. Fitting with eqs 16 and 17 reveals satisfactory results with maximum deviation from experimental data being less than a factor of 3. Although the case $(\alpha/R) = 0$ dyn/cm^2 gives mathematically slightly better results, the value $(\alpha/R) = 10^4$ dyn/cm^2 is considered the optimum fitting parameter, since in this case the model captures nicely the region of enhanced moduli and the subsequent terminal flow, observed in the experiments. This situation is depicted in Figure 14. It is noted that a parallel shift of the calculated line along the modulus axis would have made the quantitative agreement nearly perfect. It becomes evident that

(α/R) is a critical parameter which, however, depends strongly on the state of the phase-separated blend (composition and temperature). It should be noted that on the basis of the blend composition (phase diagram), the dispersed phase can be either PS-rich or PVME-rich domains. The general result is that the linear viscoelastic behavior of a phase-separated binary polymer blend resembles that of an emulsion of two incompressible viscoelastic fluids, and thus it can be described by the relevant simplified model. This suggests an analogy in terms of viscoelastic properties between the time-dependent situation of a phase-separated blend and an emulsion of incompressible viscoelastic fluids. It is therefore clear that for a higher accuracy it is imperative to improve the above assumptions and thus incorporate details of the phase-separation process into the model. In this direction, it should be mentioned that models similar to eqs 16 and 17, but with more accurate description of the contributions of morphological effects and complex interfaces to the rheological behavior of immiscible polymer blends, were recently proposed by Lee and Park[34] and Doi and Ohta[35] and were confirmed for the systems PS/linear low-density polyethylene[34] and poly(ethylene terephthalate)/nylon 6,6.[36] These works constitute the basis for future developments in this direction.

IV. Concluding Remarks

From the detailed rheological investigations of the PS/PVME blend described in this work, the following statements can be made: (i) In order to obtain adequate mixing rules over the whole concentration range (which encompasses the neighborhood of T_g as well) in the homogeneous regime, it is important to account for surface instead of the volume fractions. (ii) The thermorheological complexity of polymer blends near phase boundaries is due to large concentration fluctuations in the homogeneous regime in the vicinity of phase separation and in the various morphologies in the phase separated regime. (iii) Single shear rheological measurements suffice in order to determine both the binodal and spinodal curves. (iv) The thermorheological complexity of G' is much more pronounced than that of G''; however, the latter clearly exists. Further, the failure of TTS in polymer blends is less severe that in block copolymers near the ordering transition. (v) The magnitude of the observed effects in the vicinity of the phase boundary seems related to the dynamic asymmetry of the two constituents of the blend. (vi) In the two-phase blends, a regime of enhanced moduli (with respect to the terminal slopes) is observed and attributed to the PS-rich domains which are redistributed by the flow. (vii) The characteristic features of the viscoelastic properties of the phase-separated blends can be accounted for by a simple model describing the rheology of emulsions of two incompressible viscoelastic fluids.

Acknowledgment. This research was partially supported by the EU (Brite/Euram grant BRE2-CT-940610), NATO's Scientific Affairs Division in the framework of the Science for Stability Programme, and the Greek Secretariat of Research and Technology. We are also grateful to the Max-Buchner-Forschungsstiftung for a stipend.

References and Notes

(1) Han, C. D. *Multiphase Flow in Polymer Processing*; Academic Press: New York, 1981.
(2) Min, K.; White, J. L.; Fetters, L. J. *J. Appl. Polym. Sci.* **1984**, *29*, 2117; Han, J. H.; Choi-Feng, C.; Li, D.-J.; Han, C. D. *Polymer* **1995**, *36*, 2451.
(3) Kitade, S.; Takahashi, Y.; Noda, I. *Macromolecules* **1994**, *27*, 7397; Takahashi, Y.; Suzuki, H.; Nakagawa, Y.; Noda, I. *Macromolecules* **1994**, *27*, 6476.
(4) Mani, S.; Malone, M. F.; Winter, H. H. *J. Rheol.* **1992**, *36*, 1625.
(5) Ajji, A.; Choplin, L.; Prud'homme, R. E. *J. Polym. Sci.:Part B: Polym. Phys.* **1991**, *29*, 1573. Stadler, R.; de Lucca Freitas, L.; Krieger, V.; Klotz, S. *Polymer* **1988**, *29*, 1643.
(6) Mani, S.; Malone, M. F.; Winter, H. H.; Halary, J. L.; Monnerie, L. *Macromolecules* **1991**, *24*, 5451.
(7) Fernandez, M. L.; Higgins, J. S.; Richardson, S. M. *Polymer* **1995**, *36*, 931. Nakatani, A. I.; Kim, H.; Takahashi, Y.; Matsushita, Y.; Takano, A.; Bauer, B. J.; Han, C. C. *J. Chem. Phys.* **1990**, *93*, 795. Mani, S.; Malone, M. F.; Winter, H. H. *Macromolecules* **1992**, *25*, 5671.
(8) Wolf, B. A. *Macromolecules* **1984**, *17*, 615. Horst, R.; Wolf, B. A. *Macromolecules* **1993**, *26*, 5676.
(9) Rosedale, J. H.; Bates, F. S. *Macromolecules* **1990**, *23*, 2329. Bates, F. S.; Rosedale, J. H.; Fredrickson, G. H. *J. Chem. Phys.* **1990**, *92*, 6255. Bates, F. S. *Macromolecules* **1984**, *17*, 2607.
(10) Petri, H. M.; Stammer, A.; Wolf, B. A. *Makromol. Chem. Phys.* **1995**, *196*, 1453.
(11) Tanaka, H. *Phys. Rev. Lett.* **1996**, *76*, 787.
(12) Ferry, J. D. *Viscoelastic Properties of Polymers*, 3rd ed.; Wiley: New York, 1980.
(13) Pearce, E., private communication, 1995.
(14) Koningsveld, Z.; Kleintjens, L. A.; Schoffeleers, H. M. *Pure Appl. Chem.* **1974**, *39*, 1. Enders, S.; Stammer, A.; Wolf, B. A. *Macromol. Chem. Phys.*, in press.
(15) Koningsveld, R.; Kleintjens, L. *Macromolecules* **1971**, *4*, 637.
(16) Irving, J. B. *Viscosities of Binary Liquid Mixtures: A Survey of Mixture Equations*; Report No. 630; National Engineering Laboratory: East Kilbridge, Glasgow, U.K., 1977.
(17) Mertsch, R.; Wolf, B. A. *Ber. Bunsenges. Phys. Chem.* **1994**, *98*, 1275.
(18) Bondi, A. *J. Phys. Chem.* **1964**, *68*, 441.
(19) Ajji, A.; Choplin, L. *Macromolecules* **1991**, *24*, 5221.
(20) Fredrickson, G. H.; Larson, R. G. *J. Chem. Phys.* **1987**, *86*, 1553.
(21) Vlassopoulos, D. *Rheol. Acta*, in press.
(22) Han, C. D.; Yang, H. H. *J. Appl. Polym. Sci.* **1987**, *33*, 1199.
(23) Han, C. D.; Baek, D. H.; Kim, J. K.; Ogawa, T. Sakamoto, N.; Hashimoto, T. *Macromolecules* **1995**, *28*, 5043.
(24) Nesarikar, A. *Macromolecules* **1995**, *28*, 7207.
(25) De Gennes, P. G. *Scaling Concepts in Polymer Physics*; Cornell University Press: Ithaca, New York, 1979.
(26) Binder, K. *J. Chem. Phys.* **1983**, *79*, 6387.
(27) Kumar, S. K.; Colby, R. H.; Anastasiadis, S. H.; Fytas, G. *J. Chem. Phys.* **1996**, *105*, 3777.
(28) Koumoutsakos, A.; Vlassopoulos, D.; Anastasiadis, S. H.; Hatzikiriakos, S. G.; Englezos, P., unpublished data.
(29) Kapnistos, M.; Vlassopoulos, D.; Anastasiadis, S. H. *Europhys. Lett.* **1996**, *34*, 513.
(30) Schwahn, D.; Mortensen, K.; Yee-Madeira, H. *Phys. Rev. Lett.* **1987**, *58*, 1544. Snyder, H. L.; Meakin, P.; Reich, S. *Macromolecules* **1983**, *16*, 757.
(31) Graebling, D.; Muller, R.; Palierne, J. F. *Macromolecules* **1993**, *26*, 320. Graebling, D.; Muller, R. *J. Rheol.* **1990**, *34*, 193.
(32) Schowalter, W. R.; Chaffey, C. E.; Brenner, H. *J. Colloid Interface Sci.* **1968**, *26*, 152. Choi, S. J.; Schowalter, W. R. *Phys. Fluids* **1975**, *18*, 240.
(33) Oldroyd, J. G. *Proc. R. Sco. London* **1953**, *A218*, 122.
(34) Lee, H. M.; Park, O. O. *J. Rheol.* **1994**, *38*, 1405.
(35) Doi, M.; Ohta, T. *J. Chem. Phys.* **1991**, *95*, 1242.
(36) Guenther, G. K.; Baird, D. G. *J. Rheol.* **1996**, *40*, 1.

MA960835N